Vapor−Liquid Equilibrium Data for Binary Systems Consisting of Either Hexafluoropropene (HFP) or 2,2,3-Trifluoro-3-(trifluoromethyl)oxirane (HFPO) with Carbon Dioxide (R-744) or 2,2-Dichloro-1,1,1-trifluoroethane (R-123)

W. M. Nelson,[†] S. C. Subramoney,[†] A. Valtz,[‡] C. Coquelet,[†,‡] D. Richon,[‡] P. Naidoo,[†] and D. Ramjugernath*[,†]

Thermodynamics Research Unit, School of Chemical Engineering, Howard College Campus, University of KwaZulu-Natal, King George V Avenue, 4041 Durban, South Africa, and Centre d'Energétique, MINES ParisTech, CEP/TEP, 35 Rue Saint Honoré, 77305 Fontainebleau, France

Isothermal vapor−liquid equilibrium (VLE) data for the binary systems R-744 + HFP and R-744 + HFPO were measured at (273.15 and 313.15) K and pressures up to 5.6 MPa. Measurements were also undertaken for the HFP + R-123 and HFPO + R-123 systems at (313.15 and 333.15) K and pressures up to 1.5 MPa. The VLE data were measured via the "static-analytic" method using a fixed-volume equilibrium cell equipped with a pneumatic ROLSI sampler. The measured data have maximum uncertainties of 0.045 K and 0.003 MPa in temperature and pressure, respectively, while the relative uncertainties in the equilibrium phase analyses are within 1 % for the molar compositions. The experimental data were correlated using the Peng−Robinson equation of state with the Mathias−Copeman α function and the Wong−Sandler mixing rules incorporating the NRTL activity coefficient model.

Introduction

The Montreal Protocol[1] has mandated the replacement of ozone-depleting hydrochlorofluorocarbons (HCFCs) by the year 2030, and therefore, suitable replacement refrigerants and solvents must be identified. Vapor−liquid equilibrium (VLE) data play a crucial role as a filtering mechanism in this replacement procedure, and consequently, there is a need for reliable and accurate experimental VLE data.

Of particular interest in this study is the separation of the two close-boiling fluorochemicals hexafluoropropene (HFP) and 2,2,3-trifluoro-3-(trifluoromethyl)oxirane (HFPO). The separation of HFP and HFPO is generally enhanced by using fluorine- and chlorine-containing extractive solvents, which are affected by the HCFC phaseout. The amount of currently available VLE data for binary systems consisting of these two fluorochemicals is limited.

HFP, also known as R1216, is a colorless, odorless, and nonflammable gas at room temperature. An important application of HFP is the production of copolymers. HFP is also used to produce HFPO by oxidation.[2] HFPO is a colorless, nonflammable, stable gas at room temperature. HFPO is the most important perfluorinated epoxide because of its high reactivity, making it a versatile precursor for other fluorinated compounds.[3] Its commercial uses include the synthesis of hexafluoroacetone, high-molecular-mass perfluoroethers, and fluorinated vinyl ethers.[2]

2,2-Dichloro-1,1,1-trifluoroethane (R-123) is commonly used in refrigerant systems because of its passive nature and good refrigerant efficiency. It is also used as a solvent to separate fluorochemicals, and a patent for the separation of HFP and HFPO was filed in 1997 by the Asahi Glass Company.[4]

* Corresponding author: Tel: +27-031-2603128. Fax: +27-031-2601118. E-mail: ramjuger@ukzn.ac.za.
[†] University of KwaZulu-Natal.
[‡] MINES ParisTech.

Table 1. Specifications for Chemicals Used in This Study

component	CAS number	supplier	volume fraction
HFP	116-15-4	Interchim/Boc Edwards	0.995
HFPO	428-59-1	Interchim/Boc Edwards	0.99
R-744	124-38-9	Air Liquide	0.99995
R-123	306-83-2	Dehon	0.995

Currently, R-123 is scheduled to be phased out of production according to the Montreal Protocol by the year 2030 in industrialized countries and 2040 in developing countries. However, the possibility exists that R-123 may be granted exemption from the phaseout because of its passive nature.

The use of supercritical solvents is becoming increasingly more prominent in industrial applications. Carbon dioxide (R-744) is one of the most popular supercritical fluids because of its comparatively low critical temperature and critical pressure. R-744 is a widely popular solvent, as it is environmentally benign, inexpensive, nontoxic, and nonflammable.

VLE data were therefore measured for the systems of interest to determine whether carbon dioxide or R-123 could be potential stripping agents for the separation of HFP and HFPO.

Experimental Section

Chemicals. The four compounds HFP, HFPO, R-744, and R-123 were used in the measurements without further purification. The purity of the chemicals and the supplier information are presented in Table 1.

Apparatus. The apparatus used in this work incorporated the "static-analytic" measurement principle, similar to that described by Laugier and Richon.[5] The entire apparatus (Figure 1) was housed in a fume cupboard and consisted of an equilibrium cell submerged inside a thermally regulated liquid bath. Temperature and pressure readings of the equilibrium cell were recorded in real time through the use of a data acquisition unit. A single mobile pneumatic rapid online sampler−injector (ROLSI) sampler[6] was used to withdraw vapor and liquid samples from

10.1021/je100841y
Published on Web 12/08/2010

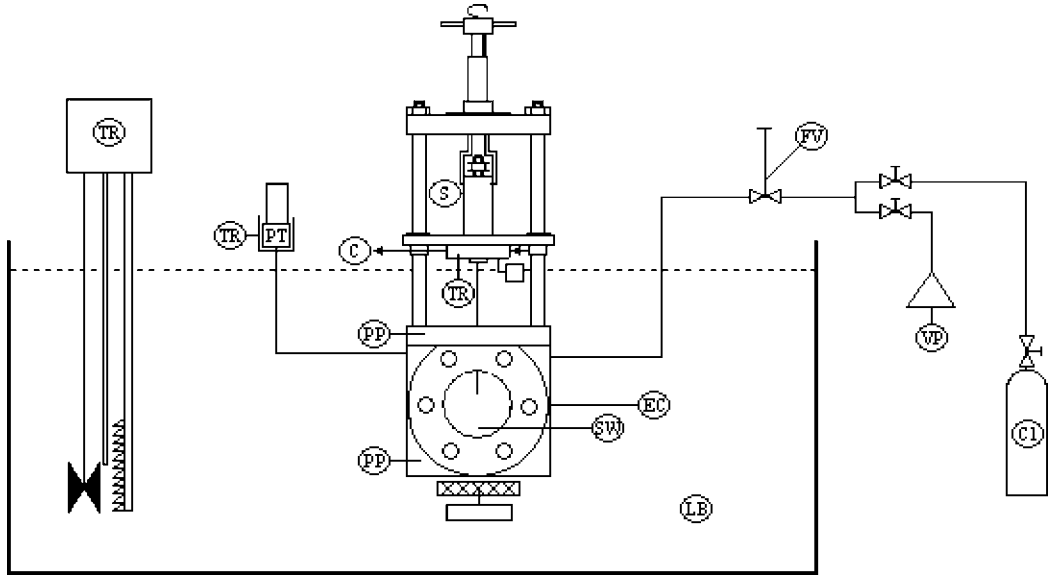

Figure 1. Schematic of the static-analytic apparatus. Legend: C, carrier gas; EC, equilibrium cell; S, ROLSI sampler; FV, feeding valve; LB, liquid bath; PP, platinum probe; C1, component 1 cylinder; PT, pressure transducer; SW, sapphire window; TR, thermal regulator; VP, vacuum pump.

the mixture in the equilibrium cell. The samples were passed through a temperature-regulated transfer line to the thermal conductivity detector (TCD) gas chromatograph (GC) for composition analysis.

The equilibrium cell, which was constructed of a titanium alloy, contained a sapphire window that allowed the direct observation of the cell contents. The attainment of equilibrium and transition of phases in the equilibrium cell was accelerated by internal magnetic stirrers. The temperature of the equilibrium cell was maintained by submerging the cell in a thermally regulated liquid bath. The bath temperature was adjusted through an external temperature regulator and also contained an external mixing device to ensure even distribution of heat throughout the bath.

For accurate and precise temperature measurement in the equilibrium cell and the ability to observe potential temperature gradients, two platinum resistance thermometers (Pt-100) were inserted inside wells drilled into the body of the equilibrium cell. One was inserted near the top of the cell and the other near the base of the cell. The probes were calibrated against a 25 Ω reference platinum resistance thermometer (Tinsley Precision Instruments) that had been calibrated by LNE (Paris) following the ITS 99 protocol.

In the apparatus, two pressure transducers were directly connected to the equilibrium cell. For low-pressure measurements, a pressure transducer [Druck model 306, type PTX611, range (0 to 0.6) MPa] was used. High-pressure measurements were also recorded using a pressure transducer [Druck model 307, type PTX611, range (0 to 6) MPa]. In order to obtain accurate pressure measurements, the pressure transducers were maintained at 353 K (a temperature higher than the highest temperature used in the study) using a device designed at the TEP Laboratories (Ecole des Mines de Paris) consisting of an air thermostat thermally controlled by a PID regulator (West Instruments, model 6100). The pressure transducers were calibrated against a dead-weight pressure balance (Desgranges & Huot, model 5202S).

With the instruments and calibration procedures used, the maximum uncertainties in the measurements of temperature and pressure were 0.045 K and 0.003 MPa, respectively.

A Hewlett−Packard online data acquisition unit (model HP34970A) directly linked to a desktop computer through an RS-232 interface was used to record all of the temperature and pressure measurements throughout the study. The data acquisition unit was set to record a single pressure and temperature measurement each second, allowing real-time temperature and pressure readings.

The analytical measurement of the vapor and liquid samples was undertaken using a gas chromatograph (Varian model CP-3800) equipped with a thermal conductivity detector. All of the peak integrations were done using Borwin version 1.5 software (JMBS, Le Fontanil, France) on a desktop computer. The analytical column used was a Porapack Q column with 80/100 mesh (1/8 in. wide, 3 m length). The GC oven temperatures were (423.15 and 473.15) K for the carbon dioxide and R-123 systems, respectively, while the injector and detector temperatures were (393.15 and 423.15) K, respectively, for all systems.

Experimental Procedure. HFP, HFPO, and R-123 were thoroughly degassed to ensure the removal of all incondensable impurities. The equilibrium cell and all loading lines were evacuated at room temperature to at least 0.1 Pa. The liquid bath temperature was reduced to around 283 K to enhance component transfer to the equilibrium cell. The first component (either HFP or HFPO) was loaded directly by gravity into the equilibrium cell. Depending on the binary system to be measured, R-744 or R-123 was added in a step-by-step manner to the equilibrium cell, with each successive step leading to an increased concentration of either R-744 or R-123 and therefore a new equilibrium mixture (R-123 was introduced via a thermal press). After each addition of either R-744 or R-123, equilibrium was assumed to be reached when the pressure remained unchanged (within ±1 kPa) for a period of 10 min under sufficient stirring. At least five samples of both the liquid and vapor phases for each equilibrium condition were withdrawn using the ROLSI sampler and checked for repeatability.

Correlations. The critical temperature (T_c), critical pressure (P_c), and acentric factor (ω) for each of the pure components are listed in Table 2. The critical properties of HFP and HFPO were obtained from the work of Subramoney et al.,[7] while those of R-744 and R-123 were obtained from the Prosim Component Plus database.[8] All of the experimental VLE data were correlated using the Thermopack software[9] developed by Armines/Ecole des Mines de Paris. The regression technique involved the $\phi-\phi$ method of data correlation using the Peng−Robinson

Table 2. Critical Property Parameters and Acentric Factors

Component	T_c/K	P_c/MPa	ω
HFP[a]	368.00	2.900	0.2046
HFPO[a]	359.15	2.926	0.2925
R-744[b]	304.21	7.383	0.2236
R-123[b]	461.60	3.610	0.2410

[a] Data from ref 7. [b] Data from ref 8.

Table 3. Regressed Model Parameters for the Measured Binary Systems on the Two Isotherms Using the PR EoS, the MC α Function, the WS Mixing Rules (k_{12}), and the NRTL Activity Coefficient Model (τ_{21} and τ_{12})

system	T/K	τ_{12}/J·mol^{-1}	τ_{21}/J·mol^{-1}	k_{12}
R-744 (1) + HFP (2)	273	6752.7	−1514.3	0.2067
	313	3683.3	−1356.1	0.3205
R-744 (1) + HFPO (2)	273	5850.0	−1510.0	0.2490
	313	5730.3	−1481.5	0.2576
HFP (1) + R-123 (2)	313	2124.4	459.0	−0.0331
	333	5778.9	−2735.9	0.1681
HFPO (1) + R-123 (2)	313	3848.8	2343.9	−0.1370
	333	4879.3	724.6	0.0037

Table 4. Vapor−Liquid Equilibrium Pressures and Phase Compositions for the R-744 (1) + HFP (2) System Compared with Values Obtained Using the Correlated Model (PR EoS, MC α Function, WS Mixing Rules, and the NRTL Activity Coefficient Model) (Δx and Δy are the Deviations between the Experimental and Modeled Values of the Liquid and Vapor Mole Fractions)

experimental			model		deviations	
p/MPa	x_1	y_1	x_1	y_1	Δx	Δy
			T/K = 273.15			
0.406	0.032	0.199	0.031	0.192	0.0014	0.0063
0.524	0.076	0.380	0.076	0.380	0.0000	0.0003
1.072	0.259	0.715	0.270	0.716	−0.0107	−0.0007
1.482	0.403	0.809	0.404	0.809	−0.0006	0.0004
1.992	0.575	0.875	0.571	0.878	0.0041	−0.0034
2.357	0.684	0.908	0.682	0.912	0.0020	−0.0040
2.604	0.760	0.934	0.759	0.933	0.0005	0.0016
			T/K = 313.15			
1.530	0.082	0.248	0.077	0.250	0.005	−0.002
2.111	0.188	0.379	0.181	0.443	0.007	−0.065
2.707	0.287	0.518	0.285	0.563	0.001	−0.046
3.063	0.347	0.599	0.345	0.615	0.002	−0.015
3.630	0.439	0.671	0.435	0.678	0.003	−0.007
4.557	0.572	0.758	0.571	0.753	0.001	0.005
5.620	0.703	0.814	0.709	0.814	−0.006	0.000

(PR)[10] equation of state (EoS) with the Mathias−Copeman (MC) α function[11] and the Wong−Sandler (WS) mixing rules[12] incorporating the nonrandom two-liquid (NRTL) activity coefficient model.[13] This particular thermodynamic model combination has been used extensively by previous researchers to successfully model binary systems containing fluorinated compounds as well as systems containing carbon dioxide.[14−24]

The Levenberg−Marquardt method was applied for the data reduction using a flash adjustment with the following objective function F:

$$F = \frac{100\ \%}{N_p}\left[\sum_i \left(\frac{x_{exptl,i} - x_{calcd,i}}{x_{exptl,i}}\right)^2 + \sum_i \left(\frac{y_{exptl,i} - y_{calcd,i}}{y_{exptl,i}}\right)^2\right] \quad (1)$$

where x_{exptl}, y_{exptl}, x_{calcd}, and y_{calcd} represent the experimental and calculated values of the liquid and vapor compositions, respectively, and N_p is the total number of data points (i = 1, ..., N_p).

Table 5. Vapor−Liquid Equilibrium Pressures and Phase Compositions for the R-744 (1) + HFPO (2) System Compared with Values Obtained Using the Correlated Model (PR EoS, MC α Function, WS Mixing Rules, and the NRTL Activity Coefficient Model) (Δx and Δy are the Deviations between the Experimental and Modeled Values of the Liquid and Vapor Mole Fractions)

experimental			model		deviations	
p/MPa	x_1	y_1	x_1	y_1	Δx	Δy
			T/K = 273.15			
1.050	0.257	0.727	0.257	0.722	0.000	0.005
1.590	0.426	0.827	0.431	0.835	−0.005	−0.008
2.060	0.580	0.889	0.580	0.889	0.000	0.000
2.360	0.674	0.913	0.676	0.916	−0.002	−0.003
2.610	0.752	0.936	0.754	0.935	−0.002	0.001
			T/K = 313.15			
1.418	0.063	0.191	0.064	0.220	−0.001	−0.029
2.081	0.177	0.449	0.177	0.449	0.000	−0.001
2.974	0.319	0.605	0.315	0.599	0.004	0.006
3.602	0.411	0.676	0.407	0.660	0.004	0.016
4.667	0.560	0.722	0.560	0.722	0.000	0.000

Table 6. Vapor−Liquid Equilibrium Pressures and Phase Compositions for the HFP (1) + R-123 (2) System Compared with Values Obtained Using the Correlated Model (PR EoS, MC α Function, WS Mixing Rules, and the NRTL Activity Coefficient Model) (Δx and Δy are the Deviations between the Experimental and Modeled Values of the Liquid and Vapor Mole Fractions)

experimental			model		deviations	
p/MPa	x_1	y_1	x_1	y_1	Δx	Δy
			T/K = 313.15			
0.905	0.762	0.923	0.771	0.921	−0.009	0.002
0.793	0.624	0.878	0.634	0.878	−0.010	0.000
0.675	0.484	0.827	0.482	0.826	0.003	0.000
0.602	0.393	0.788	0.392	0.790	0.001	−0.001
0.433	0.214	0.662	0.213	0.671	0.001	−0.009
			T/K = 333.15			
1.530	0.820	0.932	0.845	0.929	−0.026	0.003
1.394	0.720	0.890	0.720	0.890	0.000	0.000
1.191	0.555	0.843	0.543	0.836	0.012	0.007
0.913	0.367	0.747	0.348	0.746	0.019	0.001
0.658	0.200	0.596	0.198	0.608	0.002	−0.013
0.493	0.105	0.448	0.109	0.447	−0.004	0.000

Results and Discussion

The correlated parameters for each system corresponding to the WS mixing rules involving the NRTL activity coefficient model and the PR EoS are given in Table 3. Because of the limitation of only two measured isotherms, model parameter trends with temperature are not represented. The measured and calculated VLE data for each binary system are presented in Tables 4 to 7. The p−x−y phase equilibrium diagrams including experimental and modeled data at each temperature are presented in Figures 2 to 5. The critical locus lines are shown in Figures 6 and 7.

The results of a statistical analysis performed on the modeled VLE data, incorporating the bias and mean relative absolute deviation (MRD) for the calculation of deviations in the liquid- and vapor-phase compositions, are presented in Table 8. The bias and MRD give an indication of the agreement between the experimental and calculated data. The quality of the modeled data is therefore represented by the bias and MRD, with lower values of the bias and MRD indicating a closer fit of the modeled data to the measured data. The bias and MRD can therefore be

Table 7. Vapor−Liquid Equilibrium Pressures and Phase Compositions for the HFPO (1) + R-123 (2) System Compared with Values Obtained Using the Correlated Model (PR EoS, MC α Function, WS Mixing Rules, and the NRTL Activity Coefficient Model) (Δx and Δy are the Deviations between the Experimental and Modeled Values of the Liquid and Vapor Mole Fractions)

experimental			model		deviations	
p/MPa	x_1	y_1	x_1	y_1	Δx	Δy
			$T/K = 313.15$			
0.903	0.798	0.912	0.798	0.910	0.000	0.002
0.787	0.601	0.850	0.618	0.848	−0.017	0.002
0.711	0.485	0.808	0.492	0.811	−0.006	−0.003
0.623	0.360	0.757	0.351	0.767	0.009	−0.009
0.557	0.275	0.709	0.265	0.731	0.010	−0.022
			$T/K = 333.15$			
1.255	0.571	0.820	0.585	0.816	−0.013	0.003
1.086	0.419	0.764	0.419	0.764	0.000	0.000
0.930	0.307	0.690	0.297	0.712	0.010	−0.022
0.634	0.136	0.533	0.133	0.561	0.003	−0.028
0.455	0.057	0.345	0.060	0.383	−0.003	−0.039

used to compare the modeling ability of different thermodynamic models. The bias and MRD are defined as follows:

$$\text{bias } U = \left(\frac{100\ \%}{N_p}\right)\sum_i \left(\frac{U_{\text{exptl},i} - U_{\text{calcd},i}}{U_{\text{exptl},i}}\right) \quad (2)$$

$$\text{MRD } U = \left(\frac{100\ \%}{N_p}\right)\sum_i \left|\frac{U_{\text{exptl},i} - U_{\text{calcd},i}}{U_{\text{calcd},i}}\right| \quad (3)$$

where U is the measured property (i.e., vapor- or liquid-phase composition) and N_p is the total number of experimental data points.

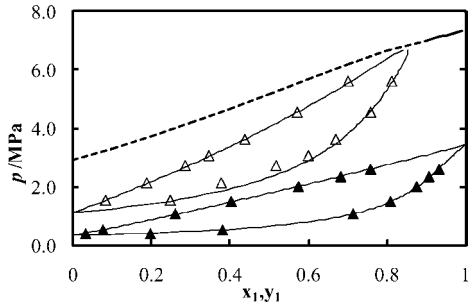

Figure 2. Modeled VLE data using the Peng−Robinson EoS with Wong−Sandler mixing rules and the NRTL activity coefficient model (solid curves) for the system R-744 (1) + HFP (2) on two isotherms: ▲, T = 273.15 K; △, T = 313.15 K. The dashed curve indicates the calculated critical line.

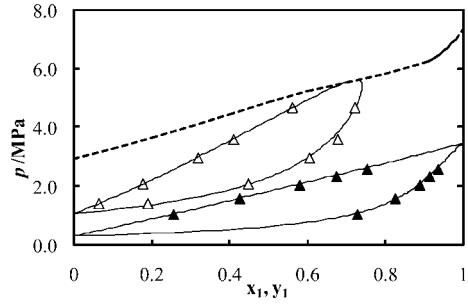

Figure 3. Modeled VLE data using the Peng−Robinson EoS with Wong−Sandler mixing rules and the NRTL activity coefficient model (solid curves) for the system R-744 (1) + HFPO (2) on two isotherms: ▲, T = 273.15 K; △, T = 313.15 K. The dashed curve indicates the calculated critical line.

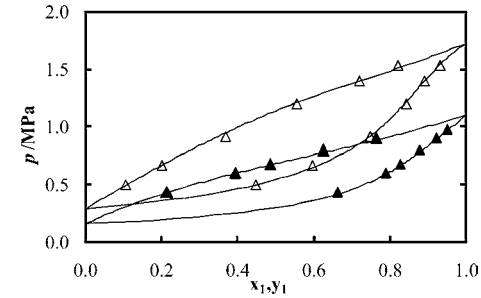

Figure 4. Modeled VLE data using the Peng−Robinson EoS with Wong−Sandler mixing rules and the NRTL activity coefficient model (solid curves) for the system HFP (1) + R-123 (2) on two isotherms: ▲, T = 273.15 K; △, T = 313.15 K.

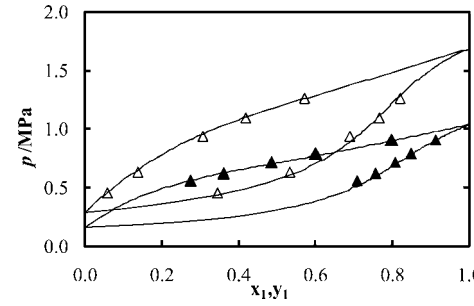

Figure 5. Modeled VLE data using the Peng−Robinson EoS with Wong−Sandler mixing rules and the NRTL activity coefficient model (solid curves) for the system HFPO (1) + R-123 (2) on two isotherms: ▲, T = 273.15 K; △, T = 313.15 K.

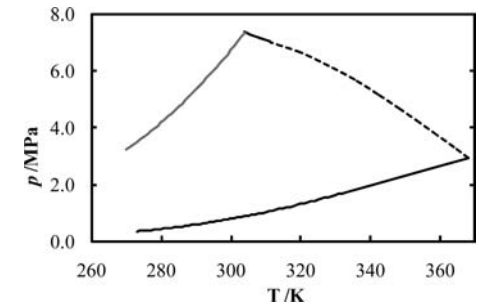

Figure 6. Critical locus lines of the R-744 (1) + HFP (2) system. The lower solid curve represents the modeled HFP vapor pressure[7] and the upper solid curve the modeled R-744 vapor pressure; the dashed curve indicates the critical locus line between the critical points of the two components.

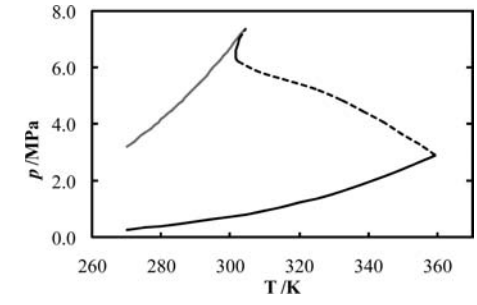

Figure 7. Critical locus lines of the R-744 (1) + HFPO (2) system. The lower solid curve represents the HFPO vapor pressure[7] and the upper solid curve the R-744 vapor pressure; the dashed curve indicates the critical locus line between the critical points of the two components.

The critical lines were calculated using the proposed procedures of Heidemann and Khalil[25] and Michelsen and Heidemann.[26] In their work, the stability criterion for an isothermal variation was assumed to be described by a minimum of the molar Helmholtz energy. The critical point corresponds to the limit of the stability. They developed an algorithm to calculate

Table 8. Statistical Analysis of the Calculated Liquid- and Vapor-Phase Compositions Represented in the Form of Bias and MRD for All of the Measured Systems

system	*T*/K	bias Δx/%	bias Δy/%	MRD Δx/%	MRD Δy/%
R-744 + HFP	273.15	0.18	1.41	0.36	0.63
R-744 + HFP	313.15	1.55	−4.24	1.81	4.44
R-744 + HFPO	273.15	−0.35	−0.10	0.35	0.42
R-744 + HFPO	313.15	0.07	−2.14	0.20	3.69
HFP + R-123	313.15	0.21	−0.20	0.84	0.28
HFP + R-123	333.15	−0.13	0.00	0.94	0.67
HFPO + R-123	313.15	0.70	−0.62	2.15	1.07
HFPO + R-123	333.15	0.77	−3.30	2.89	3.83

the critical point using a van der Waals-type EoS combined with classical mixing rules. This algorithm was generalized by Stockfleth and Dohrn[27] and was chosen in this work for the calculation of the critical loci using the PR EoS with WS mixing rules and the NRTL activity coefficient model.

Conclusion

Phase equilibrium data have been measured for four different binary systems, namely, R-744 + HFP, R-744 + HFPO, HFP + R-123, and HFPO + R-123, at two temperatures using the "static-analytic" method. The maximum uncertainties were 0.045 K and 0.003 MPa for the measurement of temperature and pressure, respectively, and within 1 % for the molar compositions.The data was regressed using the PR EoS with the WS mixing rules and the NRTL activity coefficient model. The data was very well modeled by the chosen thermodynamic model, with the computed liquid- and vapor-phase compositions generally deviating by less than 1 % from the experimental values.

Literature Cited

(1) *Montreal Protocol on Substances That Deplete the Ozone Layer*; United Nations Environment Programme, 1987.
(2) Siegemund, G.; Schwertfeger, W.; Feiring, A.; Smart, B.; Behr, F.; Vogel, H.; McKusick, B. Fluorine Compounds, Organic. In *Ullmann's Encyclopedia of Industrial Chemistry*; Wiley-VCH: Weinheim, Germany, 2007.
(3) Tarrant, P.; Allison, C. G.; Barthold, K. P.; Stump, E. C., Jr. *Fluorine Chem. Rev.* **1971**, *5*, 77–113.
(4) Toru, U.; Shin, T.; Masakuni, S.; Kenichi, E. (Asahi Glass Company Ltd.). Japanese Patent 09-020765, 1997.
(5) Laugier, S.; Richon, D. New apparatus to perform fast determinations of mixture vapor−liquid equilibria up to 10 MPa and 423 K. *Rev. Sci. Instrum.* **1986**, *57*, 469–472.
(6) Guilbot, P.; Valtz, A.; Legendre, H.; Richon, D. Rapid On-Line Sampler-Injector: A Reliable Tool for HT-HP Sampling and On-Line GC Analysis. *Analusis* **2000**, *28*, 426–431.
(7) Subramoney, S. C.; Nelson, W. M.; Valtz, A.; Coquelet, C.; Richon, D.; Naidoo, P.; Ramjugernath, D. Pure Component and Binary Vapor−Liquid Equilibrium + Modeling for Hexafluoropropylene and Hexafluoropropylene Oxide with Toluene and Hexafluoroethane. *J. Chem. Eng. Data* **2010**, *55*, 411–418.
(8) ProSim Component Plus Database, version 3, 2001.
(9) Coquelet, C.; Baba-Ahmed, A. *THERMOPACK*, version 1.10; 2005.
(10) Peng, D. Y.; Robinson, D. B. A new two parameters equation of state. *Ind. Eng. Chem. Fundam.* **1976**, *15*, 59–64.
(11) Mathias, P. M.; Copeman, T. W. Extension of the Peng−Robinson Equation of State to Complex Mixtures: Evaluation of Various Forms of the Local Composition Concept. *Fluid Phase Equilib.* **1983**, *13*, 91–108.
(12) Wong, D. S. H.; Sandler, S. I. A theoretically correct mixing rule for cubic equations of state. *AIChE J.* **1992**, *38*, 671–680.
(13) Renon, H.; Prausnitz, J. M. Local composition in thermodynamic excess function for liquid mixtures. *AIChE J.* **1968**, *14*, 135–144.
(14) Im, J.; Lee, G.; Lee, Y.-J.; Kim, H. (Vapour + liquid) equilibria of the {1,1-difluoroethane (HFC-152a) + *n*-butane (HC-600)} system. *J. Chem. Thermodyn.* **2007**, *39*, 1164–1167.
(15) Jeong, K.; Im, J.; Lee, G.; Lee, Y.-J.; Kim, H. Vapour−liquid equilibria of the carbon dioxide (CO_2) + 2,2-dichloro-1,1,1-trifluoroethane (R123) system and carbon dioxide (CO_2) + 1-chloro-1,2,2,2-tetrafluoroethane (R124) system. *Fluid Phase Equilib.* **2007**, *251*, 63–67.
(16) Valtz, A.; Gicquel, L.; Coquelet, C.; Richon, D. Vapour−liquid equilibrium data for the 1,1,1,2 tetrafluoroethane (R134a) + dimethyl ether (DME) system at temperatures from 293.18 to 358.15 K and pressures up to about 3 MPa. *Fluid Phase Equilib.* **2005**, *230*, 184–191.
(17) Valtz, A.; Coquelet, C.; Baba-Ahmed, A.; Richon, D. Vapor−liquid equilibrium data for the CO_2 + 1,1,1,2,3,3,3-heptafluoropropane (R227ea) system at temperatures from 276.01 to 367.30 K and pressures up to 7.4 MPa. *Fluid Phase Equilib.* **2003**, *207*, 53–67.
(18) Im, J.; Lee, G.; Lee, J.; Kim, H. Vapour−liquid equilibrium of the 1,1,1-trifluoroethane (HFC-143a) + dimethyl ether (DME) system. *Fluid Phase Equilib.* **2007**, *251*, 59–62.
(19) Coquelet, C.; Chareton, A.; Valtz, A.; Baba-Ahmed, A.; Richon, D. Vapor−liquid Equilibrium Data for the Azeotropic Dichloromethane + Propane System at Temperatures from 294.83 to 343.26 K and Pressures up to 5.4 MPa. *J. Chem. Eng. Data* **2003**, *48*, 317–323.
(20) Coquelet, C.; Nguyen, D.; Chareton, H. A.; Baba-Ahmed, A.; Richon, D. Vapour−liquid equilibrium data for the difluoromethane + 1,1,1,2,3,3,3-heptafluoropropane system at temperatures from 283.20 to 343.38 K and pressures up to 4.5 MPa. *Int. J. Refrig.* **2003**, *26*, 559–565.
(21) Fink, S. D.; Hershey, H. C. Modeling the vapour−liquid equilibria of 1,1,1-trichloroethane + carbon dioxide and toluene + carbon dioxide at 308, 323, and 353 K. *Ind. Eng. Chem. Res.* **1990**, *29*, 295–306.
(22) Valtz, A.; Coquelet, C.; Baba-Ahmed, A.; Richon, D. Vapour−liquid equilibrium data for the propane + 1,1,1,2,3,3,3-heptafluoropropane (R227ea) system at temperatures from 293.16 to 353.18 K and pressures up to 3.4 MPa. *Fluid Phase Equilib.* **2002**, *202*, 29–47.
(23) Shiflett, M. B.; Sandler, S. I. Modeling fluorocarbon vapor−liquid equilibria using the Wong−Sandler model. *Fluid Phase Equilib.* **1998**, *147*, 145–162.
(24) Ramjugernath, D.; Valtz, A.; Coquelet, C.; Richon, D. Isothermal Vapor−Liquid Equilibrium Data for the Hexafluoroethane (R-116) + Propane System at Temperatures from (263 to 323) K. *J. Chem. Eng. Data* **2009**, *54*, 1292–1296.
(25) Heidemann, R. A.; Khalil, A. M. The calculation of the critical point. *AIChE J.* **1980**, *26*, 769–779.
(26) Michelsen, M. L.; Heidemann, R. A. Calculation of critical point from cubic two constant equation of state. *AIChE J.* **1981**, *27*, 521–523.
(27) Stockfleth, R.; Dohrn, R. An algorithm for calculating critical points in multicomponent mixtures which can be implemented in existing programs to calculate phase equilibria. *Fluid Phase Equilib.* **1998**, *145*, 43–52.

Received for review August 16, 2010. Accepted November 8, 2010. We thank the National Research Foundation (NRF) International Science Liaison, CNRS, Pelchem, and the South African Nuclear Energy Corporation (NECSA) for financial support. This work is based upon research supported by the South African Research Chairs Initiative of the Department of Science and Technology.

JE100841Y